Proceeding Series of the Brazilian Society of Applied and Computational Mathematics, Vol. 5, N. 1, 2017.

Trabalho apresentado no CNMAC, Gramado - RS, 2016.

Proceeding Series of the Brazilian Society of Computational and Applied Mathematics

A Graph-Based Approach to Specify Perforation Placement in an Oil Reservoir Hydraulic Flow Unit

Gustavo P. de Oliveira[1]
Graduate Program in Computational and Mathematical Modelling, UFPB, João Pessoa, PB
Waldir L. Roque
Department of Scientific Computing, UFPB, João Pessoa, PB
Moises D. dos Santos
Tatiana A. Simões
Graduate Program in Mechanical Engineering, UFPB, João Pessoa, PB

Abstract. This paper brings out the applicability of graph centrality measures to suggest optimal perforation zones for oil recovery in reservoirs. Combined with a characterization technique based on HFU/FZI/DRT (Hydraulic Flow Unit/Flow Zone Indicator/Discrete Rock Type), which identifies regions with similar features of flow by means of best-fit lines and conversion formulae, the present approach analyses how the rock connectivity inside a reservoir relates to changes in the oil recovery rates. To verify the consistence of the techniques employed here, long term numerical simulations of oil recovery from perforation zones placed at locations with maximum values of closeness centrality are performed and compared, thus resulting in considerable agreement with prior conjectures.

Keywords. Reservoir Characterization, Hydraulic Flow Units, Graph Metrics, Oil Recovery.

1 Introduction

Reservoir characterization plays a fundamental role in petroleum engineering since it provides practical tools aimed to optimize processes of well placement, perforation and oil recovery. Generally, mapping the permeability field of a reservoir and locating hydraulic units for posterior production tests by means of computational simulations is a complex task which depends mainly on well core and log data. Hydraulic flow unit (HFU) is a term coined to specify a rock volume whose geological and petrophysical properties are similar and its accurate determination has been a challenge. Several researchers proposed different definitions for a HFU which are interlaced by the common ability of favouring flows. In particular, Hearn [1] says that a HFU is both a laterally and vertically continuous reservoir zone whose permeability, porosity and bedding characteristics are similar. Later, Amaefule *et al.* [2] provided a formal description that allowed the identification of HFUs in a reservoir when introducing the concepts of reservoir quality index (RQI) and flow zone indicator (FZI).

[1]gustavo.oliveira@ci.ufpb.br

Recently, a couple of different approaches based on the combination of RQI and FZI along with additional parameters like irreducible water or cementation have been proposed in the literature. Some of them included neural networks and graphs to find out HFUs from log data, as reported by [3], [4] and references therein. Nevertheless, none of these approaches have shown yet the relationship between a HFU and its oil recovery performance.

This paper brings out the applicability of the graph theory and centrality metrics to suggest optimal perforation zones for oil recovery in reservoirs. The study was performed over a synthetic field model where a small reservoir associated to a central wellbore was chosen to form a representative volume with variable discrete rock types. Interesting results concerning the rock connectivity and its effects on the choice of a wellbore reveal that the approach may provide additional parameters to detect good perforation zones. Long term numerical simulations of oil recovery rates from the predicted perforation zones are presented and compared, thus providing support to the methodology.

2 Reservoir Discretization and Base Equations

The study conducted here relies on a dataset provided by the SPE Model 2 synthetic field [5], which reconstitutes a large field. From this main volume Ω, which corresponds to a rectangular grid of $60 \times 220 \times 85$ cells, we randomly extract a subvolume described by the region $\Omega \supset \Omega^{'}(x, y, z; P) := [x - P, x + P] \times [y - P, y + P] \times [1, 85]$, where x, y are surface coordinates, z is the depth coordinate and P is a "neighbourhood radius". Let us define $w_{(x,y,z)}$ an arbitrary cell of Ω and choose the block formed from the column $W(45, 68, z) := \{w_{(45,68,1)}, \ldots, w_{(45,68,85)}\}$ with radius $P = 14$ (see Figure 1). Here, $W(45, 68, z)$ is called the well of interest and $\Omega^{'}(45, 68, z; 14)$ the volume of interest, to which we will restrict our study. For brevity, we will use the notation w_z, W and $\Omega^{'}$ for the well's cells, the well itself and the reservoir, respectively.

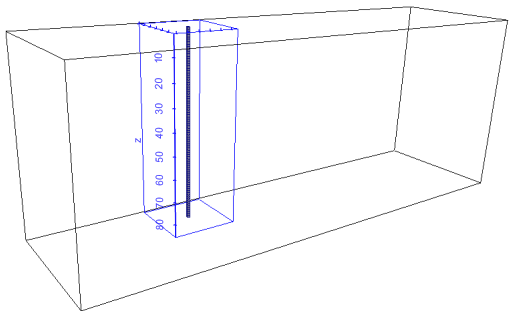

Figure 1: Overview of the domains: (a) field/reservoir/well hierarchy.

The classical Kozeny-Carman (K-C) model provides a relationship to obtain the permeability k of a porous medium from

$$k = \frac{1}{F_s \ \tau^2 \ S_{gv}^2} \frac{\phi_e^3}{(1 - \phi_e)^2}, \tag{1}$$

where ϕ_e the effective porosity, F_s the grain shape factor, τ the pore tortuosity and S_{gv} the specific surface area per grain volume. Alternatively, Amaefule *et al.* [2] defined a new form to express the K-C model as

$$\sqrt{\frac{k}{\phi_e}} = \frac{1}{\sqrt{F_s}\tau S_{gv}}\phi_z, \tag{2}$$

where $\phi_z = \frac{\phi_e}{1-\phi_e}$ is the normalized porosity. From Equation 2, the reservoir quality index (RQI) and the flow zone indicator (FZI) were defined as

$$RQI(\mu m) = 0.0314\sqrt{\frac{k}{\phi_e}}; \quad FZI = \frac{1}{\sqrt{F_s}\tau S_{gv}}, \tag{3}$$

where 0.0314 is a unit conversion factor used when k is given in milidarcies (md). Then, Equation 2 is now written as $RQI = FZI \times \phi_z$, which becomes $\log RQI = \log FZI + \log \phi_z$ after taking the logarithm on both sides. In a log-log plot of RQI versus ϕ_z, samples that lie on the same FZI line with unit slope have a common combination of attributes and form a HFU. In this line, Guo *et al.* [6] proposed a discrete rock type technique (from now on, DRT) obtained by the equation $DRT = round[2\ln(FZI) + 10.6]$, which makes the conversion from the continuous approach to the discrete one based on the pair RQI/FZI so as to allow a complete classification of the reservoir under study. Each DRT is an integer number that labels distinct HFUs.

3 Graph-Based Modelling and Data Structuring

The distribution of distinct DRT values along the well W leads to the interpretation of cells that might be identified as good HFUs. That is to say, for each $w_z \in W$, its associated value $DRT(w_z)$ is useful to indicate the set of cells that comprises a unique HFU. However, one may conjecture that one or more cells might be a good candidate to specify a perforation zone. Cells that belong to the same DRT (contiguous or spaced by a small distance) can be merged into a unique perforation zone so that, under this conjecture, the connected components around a seed-cell w_z provide a DRT-based cluster. A cluster is defined as a set $C = \{w_i; w_j,\ j, i = 1, 2, \ldots, N,\ j \neq i$, are 26-neighbour connected components of $w_i\}$ which means that any element of C does share at least on vertex, edge or face with each other. Mathematically, the transformation from a cluster C to a graph G may be described by a function $\mathcal{F}\colon \Omega^{'} \supset C \to G$ that maps each w_i to an associated node v_i linked to v_j by the edge e_{ij}. Given that, C is computationally stored as an undirected graph G whose adjacency matrix $\mathbf{M}_{adj}(G)$ of order $N \times N$ provides a node-to-node relation based on $\{0, 1\}$ wherein 1 stands for connectivity and 0 for none.

Although the well W has 85 elements, their DRT values of practical interest are limited to the set $DRT(W) := \{7, 8, 10, 11, 12, 13, 14, 15\}$. Moreover, one verifies that several cells of W belong to a same connected component due to its high predominance in $\Omega^{'}$ as seen for the $DRT = 13$, which will be studied in this paper since it corresponds to the best-fit FZIs. Figure 2, for instance, depicts the 3D view of the two biggest clusters of cells associated to

DOI: 10.5540/03.2017.005.01.0384

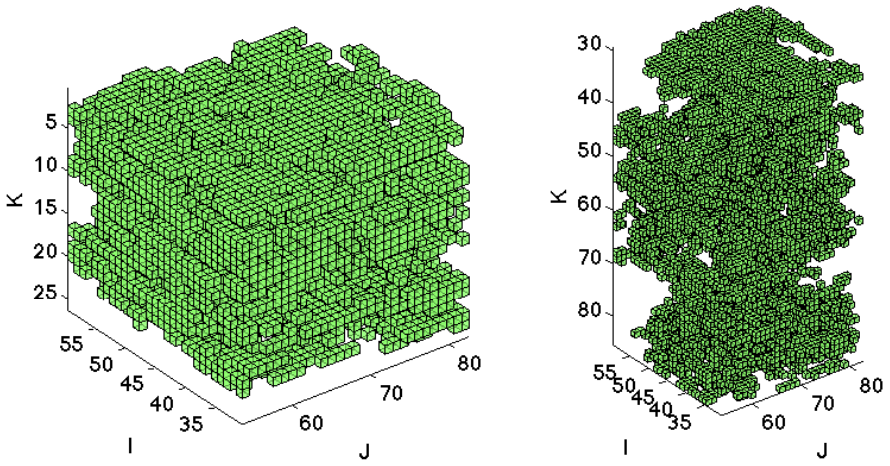

(a) (b)

Figure 2: The two biggest clusters of $DRT = 13$ that intersect W at several depths.

the $DRT = 13$. Their scaling differ because of the shape observed in each cluster as well as of their wider or narrower depth range. By labelling C_1 and C_2 these two main clusters, we have their cardinalities given respectively by $\#(C_1) = 7326$ and $\#(C_2) = 5666$ cells which, together, respond for about 18% of the reservoir volume $\Omega^{'}$. Since C_1 and C_2 are very dense, we also verify that two subsets of W, namely $W_1 = \{w_3, w_8, w_{11}, w_{12}, w_{13}, w_{14}\}$ and $W_2 = \{w_{32}, w_{40}, w_{52}, w_{58}, w_{67}, w_{70}, w_{72}, w_{73}, w_{78}, w_{79}, w_{85}\}$, gather several cells either evenly or unevenly spaced into the same connected component, i.e. $W_1 \subset C_1$ just as $W_2 \subset C_2$, besides picturing the type $DRT = 13$ into a big two-piece rock formation.

For each DRT, data structures are used to store information related to the cells and graphs that make up its components. In Figure 3, a scheme is organized to highlight a fragment of data structure (`VOISt`) used to store the volume of interest. Variables preceded by the prefix `all` (`comp`) store information of the whole group (components) of DRT, which has up to n_C clusters. The mathematical entities denoting these variables come just below in the boxes, where the encircling braces stand for a collection of arrays.

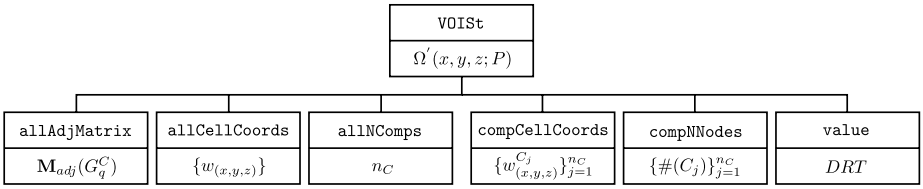

Figure 3: Fragment of computational data structure associated to a DRT.

Centralities are metrics used in graph and network theory to classify nodes and highlight special roles played by them in relation to the whole set. Here, two centrality measures are computed for each node belonging to the graphs G_1 and G_2 corresponding to the clusters C_1 and C_2, namely the closeness centrality and the degree centrality associated

to a node $v \in G_j$, $j = 1, 2$ [7] which are defined, respectively, as $\gamma(v) = 1/\sum_{i=1}^{|v|} d(v, v_i)$ and $\delta(v) = \deg(v)$, where $|v|$ is the number of nodes, $d(v, v_i)$ the shortest path distance between v and v_i, and $\deg(v)$ the degree of v which accounts for the number of edges that are connected to v. In fact, the summation above is defined as the farness property, whose reciprocal is γ. All the calculation for the individual graphs was carried on a 2.4 GHz Intel Core i5/8Gb-RAM laptop within a few minutes. Figure 4 depicts the centrality spot of γ and δ plotted over the nodes of G_j, $j = 1, 2$ as a 3D distribution through which highly concentrated regions in the γ spot as opposed to more scattered ones in the δ spot are noticed.

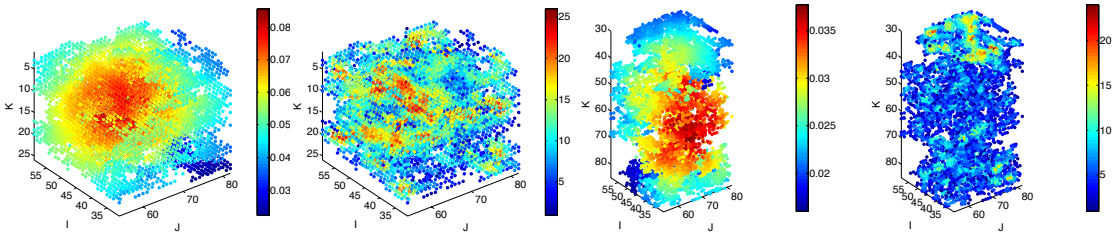

(a) $DRT = 13$; $\gamma(C_1)$ (b) $DRT = 13$; $\delta(C_1)$ (c) $DRT = 13$; $\gamma(C_2)$ (d) $DRT = 13$; $\delta(C_2)$

Figure 4: 3D distribution of γ and δ for the clusters C_1 and C_2.

In this paper, both degree and closeness centralities are assumed to establish criteria for the selection of perforation zones. While the former property describes how tightly a given facies, in the sense of a node of the graph, connects to other rocks of similar features that surround it, the latter property suggests the spatial location whence all the connectivity veins of a rock formation would be wetted by a flowing oil if a source was placed there. Table 1 summarizes the centrality data computed for the clusters C_1 and C_2. The fourth column sorts a pair of values which correspond to the maximum and minimum closeness centrality γ respectively, followed by the two values of degree centrality δ associated to these two extrema. In turn, the last column points out the cell coordinates of the respective locations inside Ω'.

Table 1: Centrality data for selection of perforation zones.

DRT	cluster	centrality	pair values	cells
13	C_1	γ	0.0858, 0.0222	(47,67,13), (32,73,25)
	C_1	δ	17, 2	
	C_2	γ	0.0378, 0.0160	(37,67,62), (46,54,85)
	C_2	δ	9, 1	

4 Numerical Simulations of Oil Recovery

To single out the validity of our approach, oil recovery factor (ORF) simulations were done and production curves were obtained from perforation zones placed exactly at the

cells whose equivalent nodes (for $j = 1, 2$) in the graphs G_j corresponded to the following sets: i) W_j, ii) $\max(\gamma)_j$, and iii) $\min(\gamma)_j$. The cells in the first set are those found at different depths of the well W whose coordinates are easily found. Yet the cells in the second and third sets are those listed in Table 1, for which we decided to take the one of minimum closeness value as a benchmark to be compared against that one of maximum closeness value in the hope of exhibiting some considerable difference. The simulations

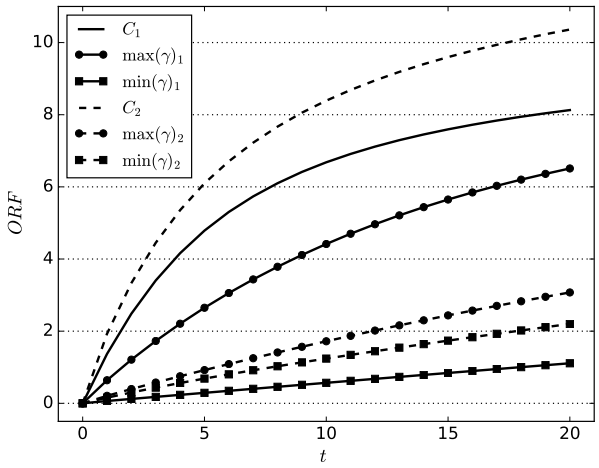

Figure 5: ORF curves in a prospect of 20 years at different perforation zones for $DRT = 13$.

considered a time range of 20 years and were performed by using the CMG® software running on a 4-node 3.20 GHz Intel Core i5/12 Gb-RAM desktop computer, whereof the respective results follow plotted in Figure 5 (solid lines for C_1; dashed lines for C_2).

We see in the plot that the ORF curves associated to the perforation zones of W_1 and W_2 dominate over the other curves of the same cluster when reaching maximum rates of about 10.36% and 8.12%, respectively. Besides, W_2 overcomes W_1 individually, possibly due to the amount of cells that form these perforation zones ($\#W_2 = 11$; $\#W_1 = 6$). As expected, the ORF curves associated to $\max(\gamma)_j$ and $\min(\gamma)_j$ evidence remarkable enhancement concerning the recovery performance with time (C_2: $ORF \approx 3.07$ % and ≈ 2.20 %; C_1: $ORF \approx 6.5\%$ and $\approx 1.11\%$). Surely, such results require deeper analyses regarding their practical advantage. Despite of that, the approach introduced here reveals that the maximum closeness cell may be a candidate to choose a good perforation zone at a given HFU.

So far, only γ was invoked to interpret the results. However, when observing the δ values associated to each cell, we can infer that the supposed perforation zones' local neighbourhoods seem to affect the results by enhancing the ORF value. In fact, each of the δ values associated to the $\max(\gamma)_j$ cells are much higher than those associated to the $\min(\gamma)_j$ cells for both clusters. This fact may indicate that their high values have some relation to the maximization of the recovery rate at those locations and suggests that the centralities may yield a set of additional parameters to be verified for the selection of promising HFUs.

DOI: 10.5540/03.2017.005.01.0384

5 Conclusions

In this paper, techniques applied to the characterization of oil reservoirs were presented with focus on computational and numerical sights. The influence of the connectivity of a rock formation in a synthetic reservoir was investigated by using computational strategies. We argued that the estimation of metrics, mainly the centrality measurements exposed here, may be relevant features to be observed in the study of reservoir characterization when combining graph theory and discrete rock typing, which together with the connectivity, may improve the identification of optimal HFUs. Although the results presented here are quite promising, additional studies are still required to ascertain how significant is the rock connectivity in the process of determining perforation zones accurately. Likewise, the influence of other variables, such as geologic formation, oil/gas/water mixture composition, rate of water saturation should be included in future models.

Acknowledgments

G.P.O. thanks to CAPES-Brazil for his scholarship. The authors thank to CMGL company.

References

[1] C.L. Hearn et al. Geological factors influencing reservoir performance of the Hartzog Draw Field, Wyoming. *Journal of Petroleum Technology*, 36(08):1–335, 1984.

[2] J.O. Amaefule et al. Enhanced reservoir description: using core and log data to identify hydraulic (flow) units and predict permeability in uncored intervals/wells. In *SPE Annual Technical Conference and Exhibition*. Society of Petroleum Engineers, 1993.

[3] A. Mirzaei-Paiaman, H. Saboorian-Jooybari, and P. Pourafshary. Improved method to identify hydraulic flow units for reservoir characterization. *Energy Technology*, 2015.

[4] M. Nouri-Taleghani, A. Kadkhodaie-llkhchi, and M. Karimi-Khaledi. Determining hydraulic flow units using a hybrid Neural Network and Multi-Resolution Graph-based Clustering method: Case study from South Pars gasfield, Iran. *Journal of Petroleum Geology*, 38(2):177–191, 2015.

[5] M.A. Christie and M.J. Blunt. Tenth SPE comparative solution project: A comparison of upscaling techniques. In *SPE Reservoir Simulation Symposium*. Society of Petroleum Engineers, 2001.

[6] G. Guo et al. Rock typing as an effective tool for permeability and water-saturation modeling: a case study in a clastic reservoir in the Oriente Basin. In *SPE Annual Technical Conference and Exhibition*. Society of Petroleum Engineers, 2005.

[7] M.E.J. Newman. *Networks: An Introduction*. Oxford University Press, New York, 2010.

